Atmospheric Research 150 (2014) 12–20

Contents lists available at ScienceDirect

Atmospheric Research

journal homepage: www.elsevier.com/locate/atmos

The growth of ice particles in a mixed phase environment based on laboratory observations

Nesvit E. Castellano [a], Eldo E. Ávila [a,*], Rodrigo E. Bürgesser [a], Clive P.R. Saunders [b]

[a] FaMAF, Universidad Nacional de Córdoba, IFEG-CONICET, Córdoba, Argentina
[b] School of Earth, Atmospheric and Environmental Sciences, University of Manchester, Manchester, UK

ARTICLE INFO

Article history:
Received 5 December 2013
Received in revised form 10 July 2014
Accepted 11 July 2014
Available online 18 July 2014

Keywords:
Ice crystal
Droplet
Mixed-phase
Cloud

ABSTRACT

This paper describes new laboratory observations about the size evolution of ice crystals and cloud droplets immersed in a mixed-phase cloud. The experiments were performed by using a cloud chamber facility for three temperatures −6 °C, −10 °C and −20 °C, in order to explore the basic crystal growth habits (columns and hexagonal plates). The sizes of the cloud droplets, ice-columns and hexagonal ice-plates were examined for growth times between 50 and 300 s. The results show evidence that after ice crystal nucleation, the cloud droplets reduce gradually their sizes by the evaporation process; while the ice crystals grow as a consequence of the water vapor diffusion process. The ice crystal growths at different temperatures were compared with the results reported by other authors. The experimental data were also compared with a theoretical model of the growth rate of ice crystals. It was observed that the numerical model provides a description of the ice columns' growth in fairly good agreement with the laboratory observations, while it predicts that the hexagonal plates evolve with maximum sizes larger than those observed in the experiments. In general, it has been noted that the results obtained from the model are very sensitive to the parameter that denotes the ratio between the condensation coefficient for the basal face and prism face. It is a critical coefficient that needs to be carefully addressed in cloud modeling.

1. Introduction

Mixed-phase clouds are an important part of the atmosphere and climate system. Detailed knowledge of the microphysical behavior of mixed-phase clouds is important for understanding the ice evolution, the precipitation development, and lifetimes of clouds. Important experimental efforts concerning the understanding of cloud processes have been made in the past few years (Pitter and Finnegan, 2010; Santachiara et al, 2010; Baumgardner et al, 2011, 2014; Cziczo and Froyd, 2014). After formation on ice nuclei, individual ice crystals grow by vapor deposition to a critical size before they can begin the riming process by collection of supercooled cloud droplets (Pruppacher and Klett, 1997; Young, 1993; Shen et al., 2014). Ávila et al. (2009), from laboratory experiments observed that the minimum crystal size necessary for the initial stage of capture and freezing of supercooled cloud droplets by hexagonal plates was around 60 μm diameter and 30 μm width and 60 μm length for columnar ice crystals.

The importance of finding an efficient representation of the ice crystal growth was recognized very early in cloud modeling. Several studies, including in-situ measurements, laboratory work and theoretical calculations, have been carried out in order to find parameterizations of the time evolution of the sizes and mass of the ice crystals as a function of the environmental variables. Ice crystal growth in supercooled cloud conditions has been studied by a number of authors in the laboratory (Mason, 1953; Fukuta, 1969; Ryan et al., 1974,1976; Takahashi and Fukuta, 1988;

* Corresponding author at: FAMAF, Ciudad Universitaria, 5000 Córdoba, Argentina.

http://dx.doi.org/10.1016/j.atmosres.2014.07.010
0169-8095/

Takahashi et al., 1991; Song and Lamb, 1994; Kikuchi et al., 2013, among others).

Mason (1953) measured the growth rates of ice crystals for hexagonal plates in the temperature range 0° to −5 °C and on prisms found between −5° and −10 °C. Fukuta (1969) measured the growth rates and fall velocities of freely falling ice crystals in a supercooled fog. Ryan et al. (1974, 1976) used a large fog chamber and measured the growth rates of ice crystals for times between 50 and 150 s. Takahashi et al. (1991) documented the crystal fall velocities and growth rates for growth times from about 3 to 30 min and for temperatures from −3° to −23 °C by reaching crystal mm-sizes. Song and Lamb (1994) studied the ice crystal growth by vapor deposition for growth times up to 4 min and temperatures between −6° and −16 °C.

The set of data that covers a broad range of supercooled cloud conditions is those from Ryan et al. (1976) and Takahashi et al. (1991). The measurements from Ryan et al. (1976) have been used by Westbrook and Heymsfield (2011) to test the theoretical model for the growth rate of simple ice crystal forms given by Houghton (1950) and Mason (1953). They conclude that the capacitance model is fairly good for modeling the early stages of crystal growth where the ventilation factor is not very important. However, in order to use this model it is necessary to have good parameterizations of the size, shape and terminal velocity of the crystals. In fact, this model only predicts the mass of crystals and not their forms. The measurements from Takahashi et al. (1991) have been used by Sheridan et al (2009) and Sulia and Harrington (2011) to check the theoretical model proposed by Chen and Lamb (1994). Given the ratio between the condensation coefficient for the basal face and prism face, this model can predict the shape evolution of the ice crystals. The main results of the experimental studies are described in more depth in the rest of this work, along with details on how they were performed.

The present work aims to obtain further knowledge of the microphysical behavior in mixed-phase clouds. The goal is to understand what happens to growth rates when ice crystals and cloud droplets coexist. A cloud chamber facility has been used in a study of ice crystal growth in supercooled clouds at three different temperatures, where basic crystal growth habits are developed (columns and hexagonal plates). The time evolution of the sizes of the cloud droplets and ice crystals are analyzed. The data are compared with past experimental data and evaluated in terms of the theoretical model proposed by Chen and Lamb (1994).

2. Experimental device

A number of experiments in the temperature range from −6 °C to −24 °C were conducted in a cloud chamber, which consisted of a vertical tube of 10 m length and 1 m inner diameter, this tube is placed inside three vertically stacked cold chambers with temperature control down to −50 °C. The cloud chamber facility where the experimental studies were performed is the Manchester Ice Cloud Chamber (MICC) at the University of Manchester, UK (http://www.cas.manchester.ac.uk/restools/cloudchamber/).

A supercooled cloud was formed by vapor condensation of water provided continuously by a boiler connected to a controlled power output in order to obtain the required liquid water content in the chamber. The air convection produced by the introduction of warm vapor into the base of the cloud chamber helped to mix and homogenize the temperature and liquid water content inside the cloud chamber. The temperature was continuously monitored by thermocouples placed close to the base, top and middle of the MICC and the fluctuation (both, spatial and temporal) in air temperature during a run was typically around ±0.8 °C on average. The liquid water content (LWC) was estimated by weighing the deposit of rime ice formed on a rod of 3 mm diameter mounted in a tube with airflow of 10 m s^{-1}. Considering the errors inherent in determining LWC, the uncertainty was 20%. Liquid water content samples were taken from the bottom and middle of the cloud chamber in order to check the homogeneity of the water droplet cloud.

The ice crystals were nucleated 1 m from the top of the cloud chamber by cooling a local volume of the droplet cloud with a rapid expansion of air from a compressed air source.

The following steps were followed to run an experiment:

- The cold chambers were settled at the desired temperature (T).
- The boiler introduced vapor into the base of the cloud chamber for about 20 min. The droplets filled the cloud chamber, reached thermal equilibrium with the environment and the cloud had time to come to steady water content.
- The ice crystals were nucleated and the boiler continued introducing vapor up to the end of the run.
- After nucleation, the ice crystals grew at the expense of the droplets and the vapor from the boiler and descended under the influence of gravity and convective current, falling through the supercooled water droplet cloud.
- Mixed-phase cloud samples were collected on glass slides coated with a thin film of 3% Formvar solution. Plastic replicas of the crystals were made as described by Schaefer (1956) for subsequent photography and measurement.

Taking into account the crystal number on the slides and the sampled volumes, we estimate that the crystal concentration varied between 80 and 800 l^{-1} in different experiments, which can be larger than those observed in typical clouds.

In order to study the temporal evolution of the size distributions of cloud droplets (diameter, d) and ice crystals (semi-axes a and c) box charts are used. Each box chart corresponds to a histogram as shown in Fig. 1; particularly, this box chart is an example and represents the maximum length of hexagonal ice plates. The horizontal bar inside the box gives the median size. The borders of the box indicate the size ranges for which between 25% and 75% of the total data are included. The small dashes give the 10th and 90th percentiles and the black points indicate the 5th and 95th percentiles.

3. Theoretical model

Chen and Lamb (1994) proposed a theoretical approach to calculate the evolution of the crystal shapes due to depositional growth. They considered that the growth rate is controlled by two factors. One of the factors is the difference in the depositional coefficients α_c and α_a, for growth along the c and a axes, respectively; this factor is represented by the inherent growth ratio, defined as $\Gamma(T) = \frac{\alpha_c}{\alpha_a}$. The second

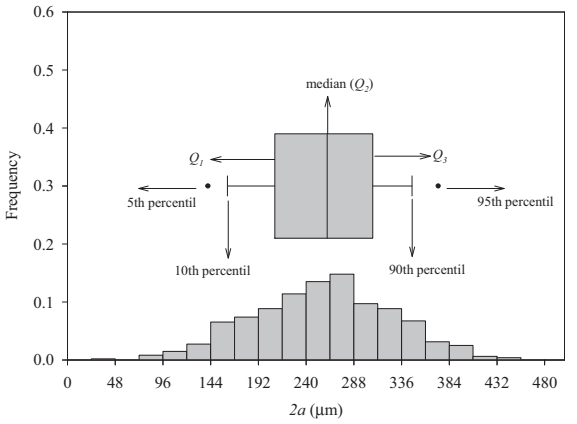

Fig. 1. Example of the box chart representing the histogram of the maximum length of hexagonal plates. The horizontal bar inside the box gives the median size. The borders of the box indicate the size ranges for which between 25% and 75% of the total data are included. The small dashes give the 10th and 90th percentiles and the black points indicate the 5th and 95th percentiles.

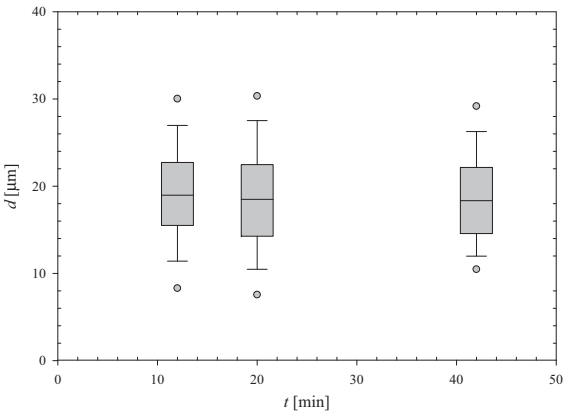

Fig. 2. Box charts of the cloud droplet size distributions as a function of time for a cloud formed at −6 °C. This cloud was prior to crystal nucleation. The numbers of sampled droplets were 1878, 1303 and 2753 for 12, 20 and 42 min, respectively.

factor is the difference in the fluxes of vapor to the prism and basal faces of the ice crystals. In fact, the vapor density gradients around irregular ice crystals are distorted by the shape of the particle.

The shapes associated with the different ice crystal habits are considered by representing hexagonal plates and column-like crystals as oblate $\left(\phi = \frac{c}{a} < 1\right)$ and prolate $(\phi > 1)$ spheroids, respectively. Thus, the rate of increase of crystal volume (V) and the primary habit evolution are parameterized as:

$$\frac{dV}{dt} = \frac{4\pi C S_i f}{\rho_{dep}\left[\frac{R_v T}{e_{i\,D_v}} + \frac{L_s}{TK_T}\left(\frac{L_s}{R_v T} - 1\right)\right]} \tag{1}$$

$$d\ln\phi = \left(\frac{\Gamma - 1}{\Gamma + 2}\right) dV \tag{2}$$

where C is the crystal capacitance, S_i is the ice supersaturation, f is the ventilation coefficient, ρ_{dep} is the effective deposition density, as parameterized by Chen and Lamb (1994) (see their Eq. (42)), R_v is the vapor gas constant, T is temperature, L_S is the enthalpy of sublimation, e_i is the ice equilibrium vapor pressure, D_v is the effective vapor diffusivity, and K_T is the effective thermal diffusivity (Pruppacher and Klett, 1997). The ventilation factor used corresponded to Hall and Pruppacher (1976), as suggested by Chen and Lamb (1994).

4. Results and discussions

In this study the growth of two basic shapes of ice crystals were analyzed, ice columns and hexagonal plates. For this reason measurements at around −6 °C, −10 °C and −20 °C were performed; the temperature interval −12 °C < T < −15 °C corresponding to dendritic growth was not considered; rimed ice crystals, aggregates and any other non-pristine ice particle habits were also disregarded from the data analysis.

The cloud droplet size distribution was characterized by taking samples at different times for a cloud free of ice crystals. Fig. 2 shows the box charts of the cloud droplet size distributions as a function of time during 42 min for a cloud formed at −6 °C. The numbers of sampled droplets were 1878, 1303 and 2753 for 12, 20 and 42 min, respectively. The results show that the droplet size distributions were quite stable in time, the sizes extend to 30 μm diameter and the average sizes are around 20 μm diameter. Similar results were found at all temperatures studied.

One of the experiments was conducted at T = −6.5 °C and liquid water content of 1 g m^{-3}, measured 120 s after ice crystal nucleation. Ice columns were the predominant habit as shown in Fig. 3. The upper picture displays an ice crystal sampled 66 s after nucleation; while the elapsed time was 239 s for the ice crystal on the lower picture.

The relationship between the length along the major axis (c-axis) and that along the minor axis (length along a-axis or width) of columnar ice crystals collected on the slides is shown in Fig. 4. Fig. 4(a), (b), (c) and (d) displays the column sizes at 66, 97, 239 and 271 s after nucleation, respectively. The numbers of sampled ice crystals were 1186 (66 s), 1049 (97 s), 1736 (239 s) and 1012 (271 s). The results show that larger ice crystals appear as time increases, indicating that they are growing in time. Although an important dispersion of the experimental data is observed in the graphs, the trend between the width and length of the columns is in general consistent with past experimental data; for instance, the solid curve shows the results obtained by Ono (1969,1970) at T = −7 °C measured for natural ice crystals. This fairly good agreement suggests that the ice crystals formed in the lab could be representative of natural ice crystals in clouds.

The temporal evolution of the lengths and widths of the columns is shown in Fig. 5(a) and (b), respectively; this Figure displays the box charts of the size distributions as a function of time. The results show that the median and percentiles of the length and width distributions expand to larger values as time passes. This Figure also shows the results obtained by Ryan et al (1976) (according to their Figs. 3 and 4) at T = −6.5 °C and Takahashi et al. (1991) for T = −5.3 °C. These are the closest experimental conditions to the current study that we found from other authors. These

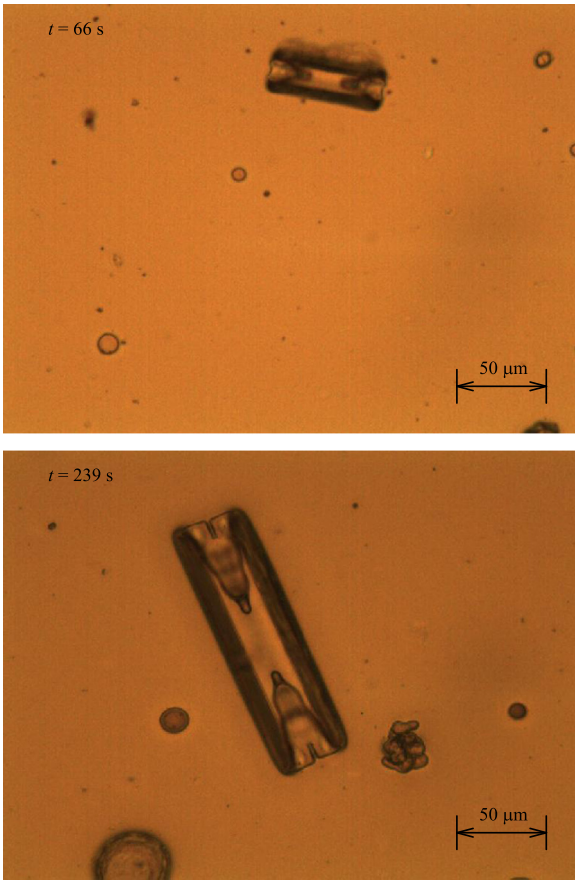

Fig. 3. Ice columns sampled 66 s (upper picture) and 239 s (lower picture) after nucleation in the experiments at T = −6.5 °C.

curves are empirical fittings from their experimental data and important discrepancies may be observed. In fact, it is possible to note that Ryan et al. (1976) found larger column lengths than the current work, for times between 50 and 150 s; while Takahashi et al. (1991) reported smaller column lengths than the current work, for times between 180 and 300 s. It looks like the present results show an intermediate trend between both previous results. On the other hand, Ryan et al. (1976) found similar column widths to the current work, for times between 50 and 150 s and Takahashi et al. (1991) reported larger column widths for times between 180 and 300 s.

The dotted lines in Fig. 5 represent the results obtained by using the theoretical model proposed by Chen and Lamb (1994); the results are obtained by integrating the columnar growth equation with the initial condition given by the first experimental data (t = 66 s). To run this model the ratio between the condensation coefficient for the basal face and prism face (Γ) needs to be predetermined. This coefficient depends on temperature and ranges between Γ = 1 and Γ = 3 for ice columns. In order to check the variability of the results for different Γ, two different Γ values were used to run the model, one of them was Γ = 2.3 as proposed by Chen and Lamb (1994) and another was Γ = 1.6 as suggested by Sei and Gonda (1989); both values were obtained from the parameterizations given by Chen and Lamb (1994) at T = −6 °C (see their Fig. 3). Substantial differences may be observed in the theoretical results, indicating that Γ is a critical parameter in the ice crystal growth equation; particularly for the column lengths. From Fig. 5 it is possible to observe that the results by using Γ = 1.6 are those that better fit the trends of column growth, as suggested by Sei and Gonda (1989).

Fig. 6 shows the results of the temporal evolution of the cloud droplet size distribution during the same experiment. The numbers of sampled droplets were 1303 (0 s), 1787 (66 s), 2635 (97 s) and 1954 (239 s). The droplet sizes are gradually reduced after ice crystal nucleation; finally, the droplets recover the original size distribution at the end of the experiments when most of the ice crystals have fallen out. These results illustrate that the droplets evaporate whereas the ice particles keep growing as a consequence of water vapor diffusing from supercooled droplets to ice crystals because the equilibrium vapor pressure over ice is lower than over liquid water at the same temperature. It is important to remark that the boiler continuously introduced vapor up to the end of the run and that the LWC = 1 g m^{-3} around 120 s; which suggests that the condition in the chamber was above ice saturation and possible slightly below water saturation, as is usual when ice crystals and droplets coexist in supercooled clouds (Castellano et al., 2008).

Another experiment with similar characteristics was carried out at T = −10.5 °C where the predominant habit was the hexagonal plate, as shown in Fig. 7 for 88 s and 193 s after nucleation. From the plastic replicas it is possible to measure the maximum dimension of the hexagonal plates (a-axis), but it is not possible to determine the plates' thickness (c-size). Fig. 8 shows the temporal evolution of the size distribution of the maximum dimension of the plates. The numbers of plates sampled in each box chart were 1132 (82 s), 970 (107 s), 1055 (131 s), 915 (162 s) and 451 (193 s). Similar to the behavior observed with the ice columns, the size distributions of the plates shifts to larger sizes as time increases. In addition to these data, the empirical results obtained by Ryan et al. (1976) and Takahashi et al. (1991) at similar temperature are shown in the Figure; within the borders of the boxes, both empirical fittings are in a reasonable good agreement with the present data. Unlike the case of ice columns, the hexagonal plates show similar crystal growth tendencies in previous and current studies.

The current data cannot be directly contrasted with the results obtained by using a theoretical model, due to the lack of the knowledge of the c-axis dimension of the hexagonal plates. Anyway, Fig. 8 displays the results from the theoretical model of Chen and Lamb (1994) using the initial conditions given by the empirical results from Ryan et al. (1976) and Takahashi et al. (1991). Again, the ice crystal growth was calculated for two different Γ values; they were Γ = 0.7 and Γ = 1 proposed by Chen and Lamb (1994) and Sei and Gonda (1989), respectively. Clearly, Γ is a significant parameter for hexagonal-plate growth and the results using Γ = 1 are those that better fit the time evolution of the hexagonal ice plates. Actually, the results show that the model predicts that the hexagonal plates evolve with maximum sizes larger than those observed in laboratory experiments. The differences between the theoretical and experimental results increase with time and can reach values

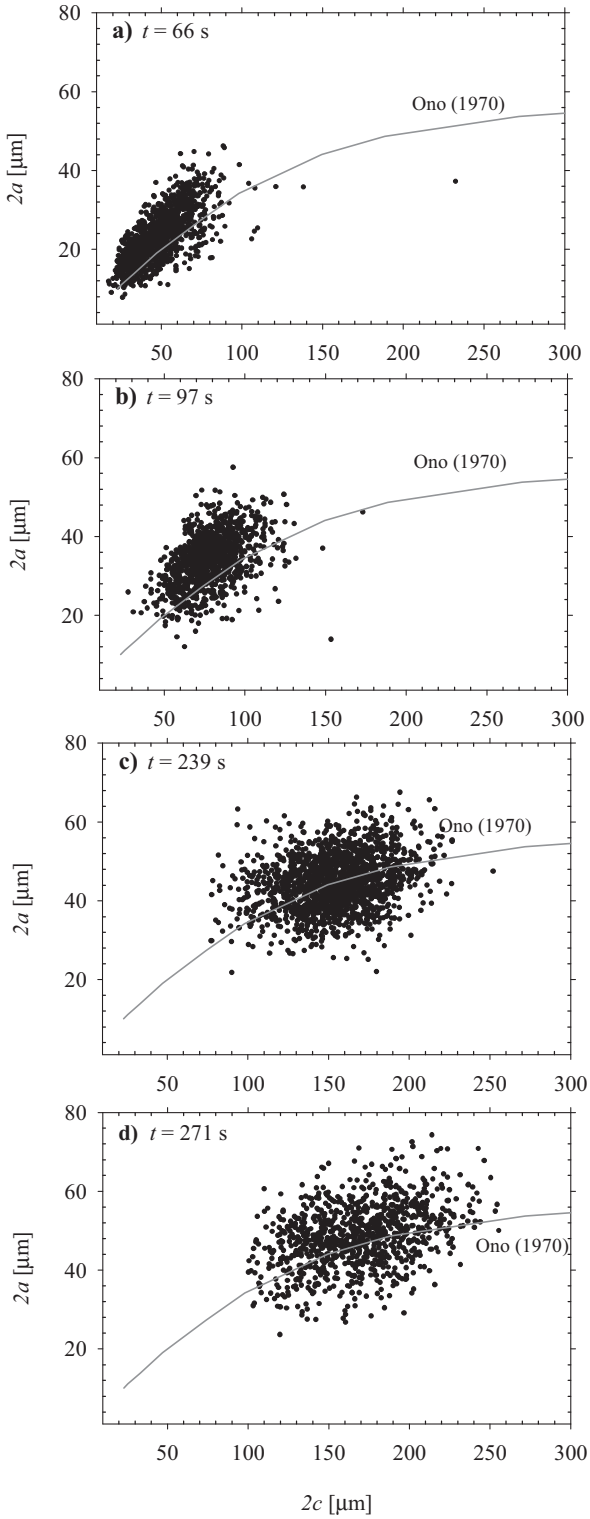

Fig. 4. The relationship between the length along the major axis and that along the minor axis (width) of columnar ice crystals collected on the slides at 66, 97, 239 and 271 s after nucleation. The numbers of sampled ice crystals were 1186 (66 s), 1049 (97 s), 1736 (239 s) and 1012 (271 s).

about 30% after 100 s. However, the results predicted by the model ($\Gamma = 1$) are within the sizes given by the border of the boxes of the results reported in this study.

Fig. 9 illustrates the temporal evolution of the cloud droplet size distribution during the experiment at T = −10.5 °C. The numbers of sampled droplets were 1303, 1627, 517 and 634 for

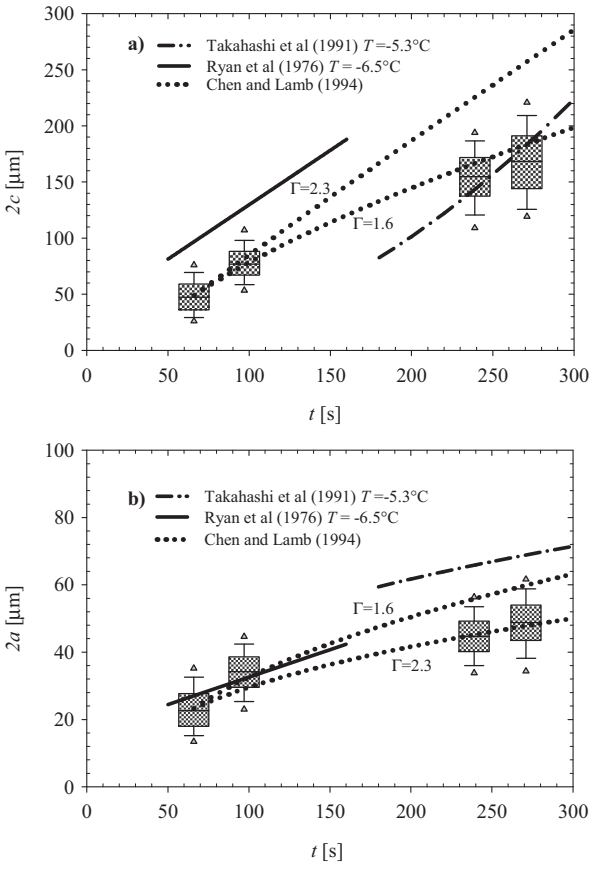

Fig. 5. Box charts displaying the temporal evolution of the length (a) and width (b) of the columns at T = −6.5 °C. The curves show the experimental results obtained by Ryan et al. (1976), Takahashi et al. (1991) and theoretical results predicted by the model by Chen and Lamb (1994).

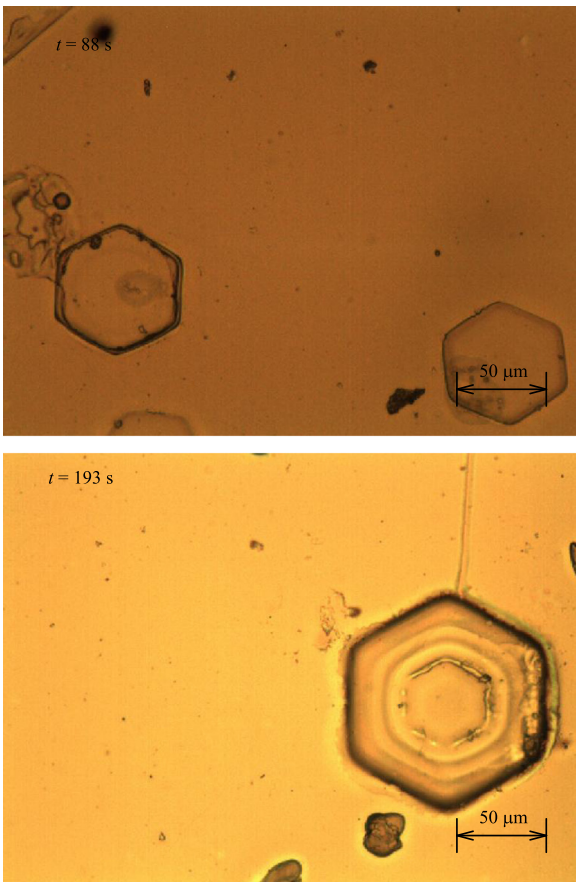

Fig. 7. Ice plates sampled 88 s (upper picture) and 193 s (lower picture) after nucleation in the experiments at T = −10.5 °C.

0, 82, 162 and 193 s, respectively. Again, it is possible to observe that the droplet sizes are reduced after ice crystal nucleation and finally they recover the original size distribution at the end of the experiments.

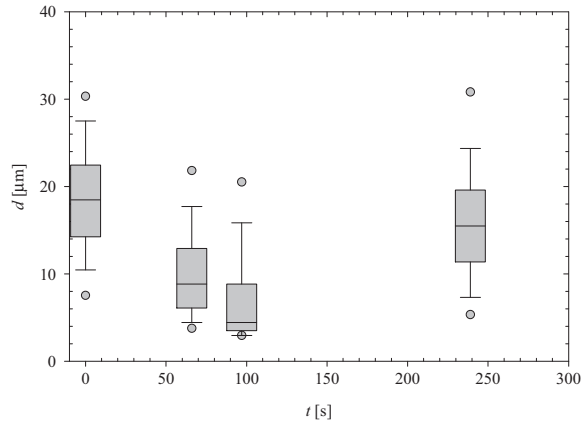

Fig. 6. The temporal evolution of the cloud droplet size distribution during the experiment at T = −6.5 °C. The numbers of sampled droplets were 1303 (0 s), 1787 (66 s), 2635 (97 s) and 1954 (239 s).

A further experiment was performed at T = −20 °C, where the hexagonal plates similar to those shown in Fig. 7 were predominant. The time evolution of the maximum dimension of the hexagonal plates is shown in Fig. 10. The numbers of sampled ice crystals were 799, 550, 94 and 397 for 84, 114, 142 and 197 s, respectively. The results obtained by Ryan et al. (1976) and Takahashi et al.(1991) at similar temperature are also shown in the same Figure. The results obtained from the theoretical model of Chen and Lamb (1994), by using the initial conditions given by the results from Ryan et al. (1976) and Takahashi et al. (1991), are displayed in Fig. 10. The coefficient Γ = 1, given by Sei and Gonda (1989) for T = −20 °C was used for the estimation. Again, the results show that the model predicts that the hexagonal plates evolve with maximum sizes larger than those observed in laboratory experiments. Particularly, the theoretical results exceed by more than 30% the experimental results of Ryan et al. (1976) for times around 150 s.

Although water vapor was continuously supplied during the experiments, the growth of an ice crystal could be reduced by the presence of neighboring crystals, mainly due to the presence of large ice crystal concentrations. Castellano et al. (2008) presented a theoretical model to calculate the vapor density field for a population of supercooled cloud droplets and ice crystals, which represents a mixed-phase

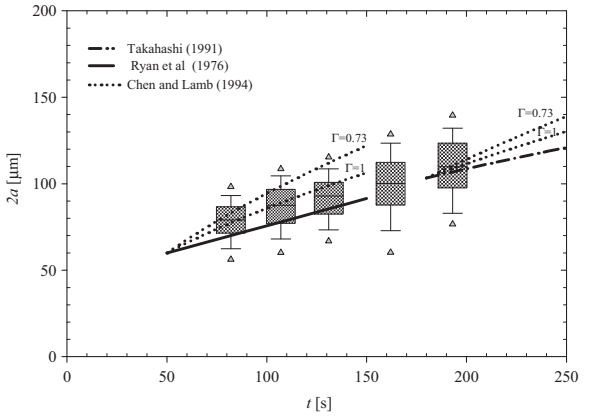

Fig. 8. Box charts displaying the temporal evolution of the maximum dimension of the hexagonal plates at T = −10.5 °C. The numbers of plates sampled in each box chart were 1132 (82 s), 970 (107 s), 1055 (131 s), 915 (162 s) and 451 (193 s). The curves show the experimental results obtained by Ryan et al. (1976), Takahashi et al. (1991) and theoretical results predicted by the model by Chen and Lamb (1994).

cloud. They gave a parameterization of the ambient vapor density (ρ_E) as a function of the sizes and concentrations of the cloud droplets and ice crystals as follow:

$$\rho_E = \rho_i + (\rho_w - \rho_i)\,\frac{bN_w}{bN_w + 1.02rN_i} \tag{3}$$

where, ρ_i and ρ_w are the vapor densities over ice and water, respectively; N_i and N_w are the number concentrations of ice crystals and droplets, respectively; r the ice crystal radius and b the cloud droplet radius. Then, the ice supersaturation may be expressed as:

$$S_i = \frac{(\rho_w - \rho_i)}{\rho_i}\,\frac{bN_w}{bN_w + 1.02rN_i}. \tag{4}$$

From the plastic samples it was possible to determine the ice crystal and droplet sizes as well as the proportion between droplet and crystal numbers. Considering that in all the experiments $N_w/N_i > 4$, we estimated the ice supersaturation for $N_w/N_i = 4$ ($S_i = S^*$) and calculated the theoretical growth rates for this value. Fig. 11 displays the experimental data for ice columns at T = −6.5 °C (Fig. 11a and b) and hexagonal plates at T = −10.6 °C (Fig. 11c) and T = −20.1 °C (Fig. 11d) together with the theoretical growth rates corresponding to the environment at water saturation ($S_i = S_w$) and ice supersaturation calculated according to Eq. (4) ($S_i = S^*$). The theoretical curves were calculated by using Γ = 1.6 and Γ = 1 for ice columns and plates, respectively. These results show the sensitivity of ice crystal growth to S_i value. It is observed that for −6.5 °C and −10.6 °C the experimental results are mainly enclosed by the theoretical curves with different S_i values. These results suggest that some ice crystals may have grown at different supersaturations; likely, due to variations in the spatial distribution of the vapor density inside the cloud chamber. This could explain, at least partially, the dispersion of the measured data.

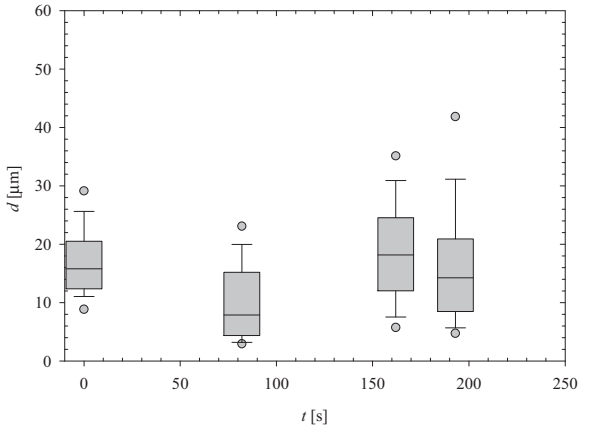

Fig. 9. The temporal evolution of the cloud droplet size distribution during the experiment at T = −10.5 °C. The numbers of sampled droplets were 1303, 1627, 517 and 634 for 0, 82, 162 and 193 s, respectively.

5. Summary and conclusions

Based on laboratory observations, the time evolutions of the cloud droplets and ice crystals were studied at different temperatures. The sizes of the cloud droplets, ice-columns and hexagonal ice-plates were examined for growth times between 50 and 300 s. The results show evidence that the mixture of liquid droplets, water vapor and ice particles coexisting at temperatures below 0 °C is a thermodynamically unstable system. In fact, after ice crystal nucleation, the cloud droplets reduce gradually their sizes by evaporation process; while the ice crystals grow as a consequence of water vapor diffusion from supercooled droplets and from the boiler. By the last part of the experiments, the cloud droplets recover the original size distribution when most of the ice crystals have fallen out.

The ice crystal growth at different temperatures was compared with the results reported by Ryan et al. (1976) for

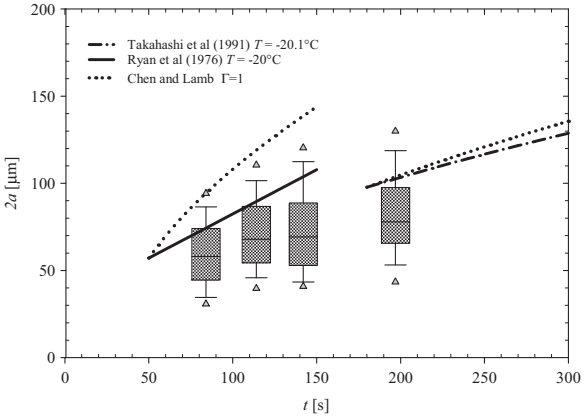

Fig. 10. Box charts displaying the temporal evolution of the maximum dimension of the hexagonal plates at T = −20 °C. The numbers of sampled ice crystals were 799, 550, 94 and 397 for 84, 114, 142 and 197 s, respectively. The curves show the experimental results obtained by Ryan et al. (1976), Takahashi et al. (1991) and theoretical results predicted by the model by Chen and Lamb (1994).

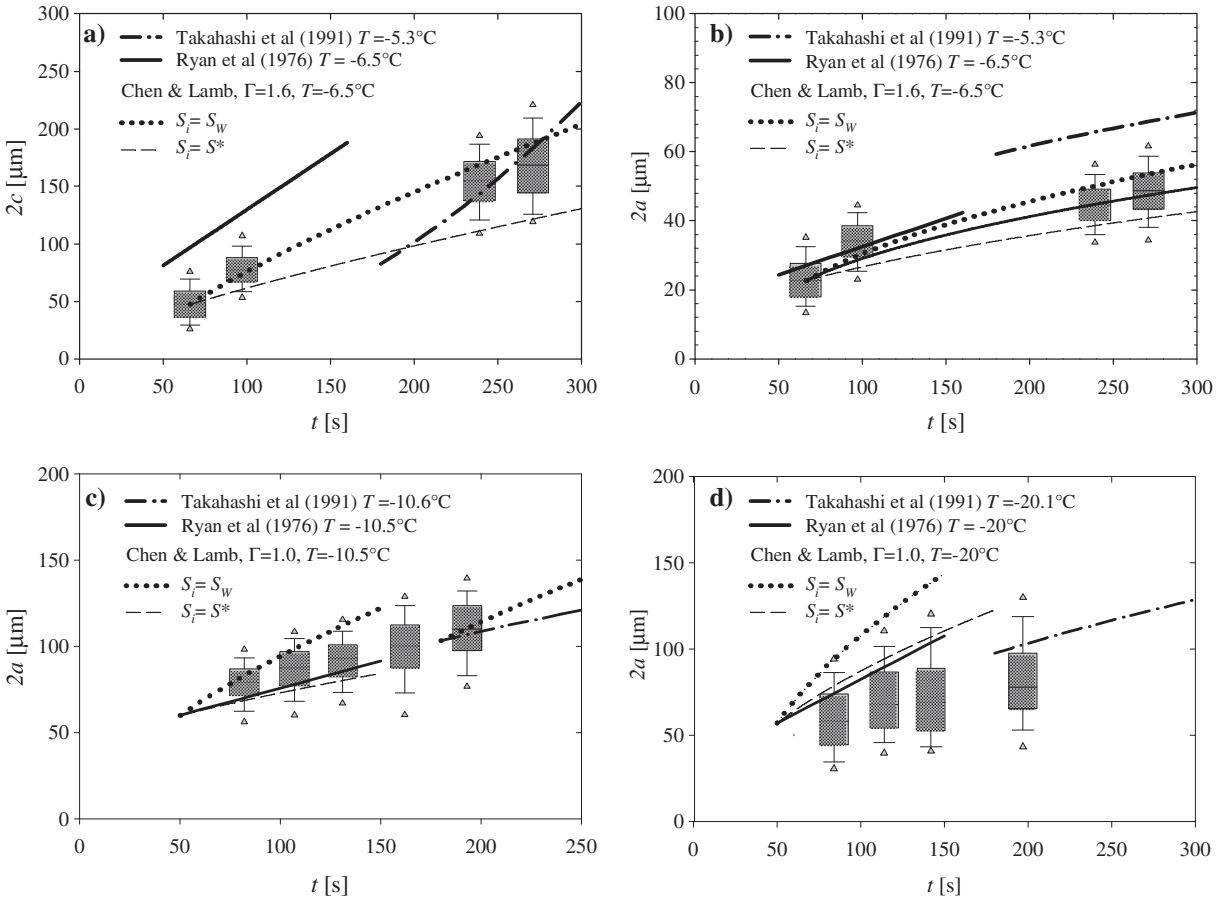

Fig. 11. Theoretical growth rates corresponding to the environment at water saturation ($S_i = S_w$) and ice supersaturation ($S_i = S^*$) together with the experimental data for ice columns at T = −6.5 °C (a and b) and hexagonal plates at T = −10.6 °C (c) and T = −20.1 °C (d).

times between 50 and 150 s and by Takahashi et al. (1991) for times between 180 and 300 s. Although the growing period of the ice crystals studied by Ryan et al. (1976) and Takahashi et al. (1991) are not superimposed, important differences are found between the tendencies of the ice columns growth of both studies. The present results show an intermediate trend between both previous results. Meanwhile, the present and previous studies show a reasonable agreement for hexagonal plate growth.

Regarding the numerical model for ice crystal growth proposed by Chen and Lamb (1994), it has been noted that the results obtained from the model are very sensitive to the parameter Γ, which denotes the ratio between the condensation coefficient for the basal face and prism face. It is a critical coefficient that needs to be carefully addressed when the model is used.

The experimental data were contrasted with the model by Chen and Lamb (1994). It was found that the results that better predict the trends of the experimental data are those that used the parameterization given by Sei and Gonda (1989) for the coefficient Γ as a function of temperature. In general, the numerical model provides a description of the ice column growth in good agreement with the laboratory observations; while it predicts that the hexagonal plates evolve with maximum sizes larger than those observed in the experiments.

Acknowledgments

This work was supported by the Secretaria de Ciencia y Tecnología de la Universidad Nacional de Córdoba (124/13), Consejo Nacional de Investigaciones Científicas y Tecnológicas (CONICET) (112-200801-02848), and Agencia Nacional de Promoción Científica y Tecnológica (FONCYT) (PICT-2010 No 826). We want to thank Peter Kelly, C. Emersic and Vanesa Alvarez for their assistance in this work.

References

Ávila, E.E., Castellano, N.E., Saunders, C.P.R., Bürgesser, R.E., Aguirre Varela, G. G., 2009. Initial stages of the riming process on ice crystals. Geophys. Res. Lett. 36, L09808. http://dx.doi.org/10.1029/2009GL037723.

Baumgardner, D., Brenguier, J.L., Bucholtz, A., Coe, H., DeMott, P., Garrett, T.J., Gayet, J.F., Hermann, M., Heymsfield, A., Korolev, A., Krämer, M., Petzold, A., Strapp, W., Pilewskie, P., Taylor, J., Twohy, C., Wendisch, M., Bachalo, W., Chuang, P., 2011. Airborne instruments to measure atmospheric aerosol particles, clouds and radiation: a cook's tour of mature and emerging technology. Atmos. Res. 102, 10–29.

Baumgardner, D., Newton, R., Krämer, M., Meyer, J., Beyer, A., Wendisch, M., Vochezer, P., 2014. The Cloud Particle Spectrometer with Polarization

Detection (CPSPD): a next generation open-path cloud probe for distinguishing liquid cloud droplets from ice crystals. Atmos. Res. 142, 2–14.
Castellano, N.E., Avila, E.E., Saunders, C.P.R., 2008. Vapour density field of mixed phase clouds. Atmos. Res. 88, 56–65.
Chen, J.-P., Lamb, D., 1994. The theoretical basis for the parameterization of ice crystal habits: growth by vapor deposition. J. Atmos. Sci. 51, 1206–1221.
Cziczo, D.J., Froyd, K.D., 2014. Sampling the composition of cirrus ice residuals. Atmos. Res. 142, 15–31.
Fukuta, N., 1969. Experimental studies on the growth of small ice crystals. J. Atmos. Sci. 26, 522–531.
Hall, W., Pruppacher, H.R., 1976. The survival of ice particles falling from cirrus clouds in subsaturated air. J. Atmos. Sci. 33, 1995–2006.
Houghton, H.G., 1950. A preliminary quantitative analysis of precipitation mechanisms. J. Meteorol. 7, 363–369.
Kikuchi, K., Kameda, T., Higuchi, K., Yamashita, A., 2013. A global classification of snow crystals, ice crystals, and solid precipitation based on observations from middle latitudes to polar regions. Atmos. Res. 132–133, 460–472.
Mason, B.J., 1953. The growth of ice crystals in a supercooled water cloud. Q. J. R. Meteorolog. Soc. 79, 104–111.
Ono, A., 1969. The shape and riming properties of ice crystals in natural clouds. J. Atmos. Sci. 26, 138–147.
Ono, A., 1970. Growth mode of ice crystals in natural clouds. J. Atmos. Sci. 27, 649–658.
Pitter, R.L., Finnegan, W.G., 2010. Mechanism of single ice crystal growth in mixed clouds. Atmos. Res. 97, 438–445.
Pruppacher, H.R., Klett, J.D., 1997. Microphysics of clouds and precipitation, 2nd ed. Atmos. Oceanogr. Sci. Libr, vol. 18. Kluwer Acad, Dordrecht, Netherlands (954 pp.).
Ryan, B.F., Wishart, E.R., Holroyd, E.W., 1974. The densities and growth rates of ice crystals between −5 °C and −9 °C. J. Atmos. Sci. 31, 2136–2141.
Ryan, B.F., Wishart, E.R., Holroyd, E.W., Shaw, D.E., 1976. The growth rates and densities of ice crystals between −3°and −21 °C. J. Atmos. Sci. 33, 842–850.
Santachiara, G., Di Matteo, L., Prodi, F., Belosi, F., 2010. Atmospheric particles acting as ice forming nuclei in different size ranges. Atmos. Res. 96, 266–272.
Schaefer, V.J., 1956. The preparation of snow crystal replicas-VI. Weatherwise 9, 132–135.
Sei, T., Gonda, T., 1989. The growth mechanism and the habit change of ice crystals growing from the vapor phase. J. Cryst. Growth 94, 697–707.
Shen, X., Huang, W., Qing, T., Huang, W., Li, X., 2014. A modified scheme that parameterizes depositional growth of ice crystal: a modeling study of pre-summer torrential rainfall case over Southern China. Atmos. Res. 138, 293–300.
Sheridan, L.M., Harrington, J.Y., Lamb, D., Sulia, K., 2009. Influence of ice crystal aspect ratio on the evolution of ice size spectra during vapor depositional growth. J. Atmos. Sci. 66 (12), 3732–3743. http://dx.doi.org/10.1175/2009JAS3113.1.
Song, N., Lamb, D., 1994. Experimental investigations of ice in supercooled clouds. Part 1: system description and growth of ice by vapor deposition. J. Atmos. Sci. 51, 91–103.
Sulia, K.J., Harrington, J.Y., 2011. Ice aspect ratio influences on mixed-phase clouds: impacts on phase partitioning in parcel models. J. Geophys. Res. — Atmos. 116. http://dx.doi.org/10.1029/2011JD016298.
Takahashi, T., Fukuta, N., 1988. Supercooled cloud tunnel studies on the growth of snow crystals between −4 °C and −20°. J. Meteorol. Soc. Jpn. 66 (6), 841–855.
Takahashi, T., Endoh, T., Wakahama, G., Fukuta, N., 1991. Vapor diffusional growth of free-falling snow crystals between −3 °C and −23 °C. J. Meteorol. Soc. Jpn. 69, 15–30.
Westbrook, C.D., Heymsfield, A.J., 2011. Ice crystals growing from vapor in supercooled clouds between −2.5° and −22 °C: testing current parameterization methods using laboratory data. J. Atmos. Sci. 68, 2416–2429.
Young, K.C., 1993. Microphysical Processes in Clouds. Oxford Univ, Press, New York.